Potency of Human Cardiosphere-Derived Cells from Patients with Ischemic Heart Disease Is Associated with Robust Vascular Supportive Ability

EMMA HARVEY,[a,]* HUAJUN ZHANG,[b,c,]* PILAR SEPÚLVEDA,[d]* SARA P. GARCIA,[e,f,g] DOMINIC SWEENEY,[a,c] FIZZAH A. CHOUDRY,[e,f] DELIA CASTELLANO,[d] GEORGE N. THOMAS,[b,c] HASSAN KATTACH,[b] ROMINA PETERSEN,[d,e] DEREK J. BLAKE,[h] DAVID P. TAGGART,[b] MATTIA FRONTINI,[e,f,g] SUZANNE M. WATT,[a,c] ENCA MARTIN-RENDON[a,c]

[a]Radcliffe Department of Medicine, [b]Nuffield Department of Surgical Sciences, University of Oxford, Oxford, United Kingdom; [c]R&D Division, National Health Service (NHS)-Blood and Transplant, Oxford Centre, Oxford, United Kingdom; [d]Mixed Unit for Cardiovascular Repair, Instituto de Investigación Sanitaria La Fe-Centro de Investigación Príncipe Felipe, Valencia, Spain; [e]Department of Haematology, [f]British Heart Foundation Centre of Excellence, University of Cambridge, Cambridge, United Kingdom; [g]R&D Division, National Health Service (NHS)-Blood and Transplant, Cambridge Centre, Cambridge, United Kingdom; [h]MRC Centre for Neuropsychiatric Genetics & Genomics, Cardiff University, Cardiff, United Kingdom

*Contributed equally.

Correspondence: Enca Martin-Rendon, Ph.D., FRSB, Radcliffe Department of Medicine, University of Oxford, John Radcliffe Hospital, Headington, Oxford OX3 9DU, United Kingdom. Telephone: 44 (0)7517 663838; Fax: 44 (0)1865 228980; e-mail: enca.rendon@ndcls.ox.ac.uk; encamartinrendon@gmail.com

ABSTRACT

Cardiosphere-derived cell (CDC) infusion into damaged myocardium has shown some reparative effect; this could be improved by better selection of patients and cell subtype. CDCs isolated from patients with ischemic heart disease are able to support vessel formation in vitro but this ability varies between patients. The primary aim of our study was to investigate whether the vascular supportive function of CDCs impacts on their therapeutic potential, with the goal of improving patient stratification. A subgroup of patients produced CDCs which did not efficiently support vessel formation (poor supporter CDCs), had reduced levels of proliferation and increased senescence, despite them being isolated in the same manner and having a similar immunophenotype to CDCs able to support vessel formation. In a rodent model of myocardial infarction, poor supporter CDCs had a limited reparative effect when compared to CDCs which had efficiently supported vessel formation in vitro. This work suggests that not all patients provide cells which are suitable for cell therapy. Assessing the vascular supportive function of cells could be used to stratify which patients will truly benefit from cell therapy and those who would be better suited to an allogeneic transplant or regenerative preconditioning of their cells in a precision medicine fashion. This could reduce costs, culture times and improve clinical outcomes and patient prognosis. STEM CELLS TRANSLATIONAL MEDICINE 2017;6:1399–1411

SIGNIFICANCE STATEMENT

This study aimed at developing personalized treatments for heart disease that involved stem/progenitor cells isolated from the patients' own heart. During heart surgery, a tiny piece of heart tissue was taken. Heart cells were gown in the laboratory and screened for signs that they were healthy and will be beneficial when transplanted back into the patients' heart. Cells from some patients grew well; they supported blood vessel formation and improved heart function while others did not. Our results showed that screening those cells will predict the best cells to use and the patients that will benefit most from the treatment.

INTRODUCTION

Ischemic heart disease (IHD) is the foremost cause of mortality worldwide and it is characterized by inadequate blood supply to the myocardium [1, 2]. Thus, promoting blood vessel regeneration and/or remodeling, either by administration of angiogenic factors or cell transplantation, has emerged as a new therapeutic approach in patients with IHD. Importantly, an increase in capillary density following bone marrow cell transplantation has been directly correlated with improvement in cardiac function [3]. However, risk factors associated with IHD are known to affect not only the numbers, but the mobilization, homing, and engraftment of cells, both resident in the bone marrow and mobilized into the peripheral circulation [4, 5]. Tissue-specific progenitor cells may therefore be a better alternative for cell therapy.

Currently in the cell therapy field, there is a strong interest in selecting the optimal cell type and patient population to obtain the best therapeutic response in vivo. A cardiac cell population characterized by their ability to form cardiospheres (cardiosphere-derived cells or CDCs) has been successfully isolated from the human heart by us and others [6–10]. In a head to head

comparison with bone marrow mesenchymal stromal cells (BM-MSC), adipose tissue MSC and bone marrow mononuclear cells, CDC showed a greater therapeutic ability in a rodent model of myocardial infarction (MI) [11]. Additionally, a recent systematic review of cardiac progenitor cells (CPCs) in preclinical studies established CDCs as having the highest level of therapeutic benefit in small animal models of myocardial ischemia as measured by improvement in left ventricular ejection fraction (LVEF) [12]. CDCs have been shown to have a therapeutic benefit in the intracoronary autologous CPC transfer in patients with hypoplastic left heart syndrome (TICAP) trial, improving right ventricular ejection fraction (EF) and reducing heart failure status in pediatric patients [13]. CDCs have also been administered to adult patients who have suffered a recent MI [14, 15]. While transplantation of these cells reduced infarct size and increased viable myocardium for over a year, this was not accompanied by an improvement in vessel density or in left ventricular function [14, 15]. Improving the cell selection method and the use of potency assays could improve clinical outcomes.

Blood vessel formation occurs by three main mechanisms (vasculogenesis, angiogenesis, and arteriogenesis) to which not only endothelial cells but stromal and other supportive cells are pivotal [16]. CDCs can support blood vessel formation in vivo in preclinical models of myocardial ischemia [7, 17, 18], but it is unknown if CDCs from all IHD patients will have a robust vascular supportive function. Therefore, the primary aim of our study was to investigate whether vascular supportive ability of CDCs impacts on their therapeutic potential and how this may be affected by associated risk factors or comorbidities. We also aimed at developing a functional assay that could be used as a potency assay to select the optimal cells for the right patient cohort, thus providing a means to personalizing cell therapy as treatment for IHD.

MATERIALS AND METHODS

Patients

Cardiac tissue biopsies were obtained from the right atrial appendage with informed written consent and ethical approval granted by the Berkshire Research Ethics Committee (reference 07/H0607/95) and were handled, processed, and stored under a Human Tissue Authority license (number 11042). Fifty patients undergoing cardiac surgery at the Cardiothoracic Unit, John Radcliffe Hospital, Oxford, U.K. were recruited with no restriction of age or comorbidities and providing they were not participating in other trials. The study was blinded and clinical records were accessed only to establish the multiple regression model.

Cell Culture

Isolation and culture of CDC was performed according to previously described protocols [6, 9]. CDCs were cultured on fibronectin coated (0.33 μg/cm^2) tissue culture plastic for all assays. Single donor human BM-MSC (Lonza, Slough, UK, http://www.lonza.com/) and human umbilical vein endothelial cells (HUVEC, Lonza) were grown according to the manufacturer's instructions. All cells were maintained at 37°C, 5% (vol/vol) CO$_2$ with media changes every 2–3 days.

Flow Cytometry

Expression of cell surface antigens was assessed by flow cytometry as described previously [6]. Briefly, cells were incubated with human FcR block (BD Biosciences, Oxford, UK, http://www.bd.com/uk/) at 4°C for 30 minutes, then incubated at 4°C for 30 minutes with the relevant test antibodies: CD31, CD34, CD45, CD73, CD90 (BD Biosciences), CD44 (Bio-Rad, Watford, UK, http://www.biorad.com/), CD105 (R&D Systems, Abingdon, UK, http://www.rnddsystems.com/), CD117, CD133 (Miltenyi Biotec, Bisley, UK, http://www.miltenyibiotec.com/), or isotype controls. Median fluorescent intensities and percentage positive cell populations were measured using a LSRSII flow cytometer and analysis was conducted using the FACS Diva software (BD Biosciences).

Cell Labeling

A lentiviral vector system expressing green fluorescent protein (GFP) was used to generate lentiviral particles as previously described [19]. HUVECs were transduced with lentiviral vector particles expressing GFP (LV-GFP) at a multiplicity of infection (MOI) of 3. Typical titers of the LV-GFP stocks were in the range of 6×10^6 to 2×10^7 transducing units per ml. At the MOI used, over 98% of HUVEC were transduced with no detriment to cell viability or proliferation.

Tubule Assay

1.5×10^3 GPF-labeled HUVEC, were seeded with 3×10^4 BMSC or CDCs in endothelial growth medium (EGM)−2 (Lonza) in a coculture assay as previously described [20]. Images were taken on day 14 using a Nikon TE2000-U microscope (Nikon UK Ltd, http://www.europe-nikon.com/en_GB/) with the PCI simple software (Hamamatsu Photonics, Welwyn Garden City, UK, http://www.hamamatsu.co.uk/). Image analysis to determine the total tubule length (TTL) was performed using the AngioSys software (TCS Cellworks, Buckingham, UK, http://www.cellworks.co.uk/). The coculture of GFP-HUVEC and BMSC was used as a positive control, the TTL of test CDCs relative to this control (represented as 100%) was defined as relative tubule length (RTL). The tubule formation experiments were performed routinely at CDC passage 2 and repeated as a quality control step at a later passage for some CDC samples.

For each patient, CDCs sample TTL and RTL were recorded as mean values, the samples were then ordered by these values and split into tertiles classified as: high tubule formation (first tertile), moderate tubule formation (second tertile), and low tubule formation (third tertile).

For subsequent analysis CDCs with a TTL above 4,000 were referred to as good supporters of angiogenesis and CDCs with a TTL below 4,000 were referred to as poor supporters of angiogenesis.

RNA-Sequencing

Total RNA from six CDC samples was isolated using QIAzol and RNeasy mini kits (QIAgen, Manchester, UK, http://www.qiagen.com/) according to the manufacturer's instructions and treated with DNase I (Promega, Southampton, UK, http://www.promega.co.uk/) to remove genomic DNA. Library preparation and sequencing was performed as previously described using Clontech Smart seq kit [21]. Quality control, trimming, alignment, and differential expression analysis using a Bayesian linear mixed effects model was performed as described elsewhere [21, 22] using Bowtie, MMSEQ, and MMDIF [22–24]. Differentially expressed genes and transcripts were required to have a posterior probability >0.3. The RNA-sequencing (RNA-seq) data was submitted to the gene expression omnibus, accession number GSE81827 (http://

www.ncbi.nlm.nih.gov/geo/query/acc.
cgi?token=mfupcoyovzyxdub&acc=GSE81827).

Gene Enrichment Analysis

Gene sets derived from the RNA-seq data with a posterior proba-
bility >0.3 were analyzed for gene enrichment with DAVID v6.7
[25] [26] and the top 10 significantly upregulated (p value $\leq$ .05)
terms in the molecular function (GOTERM_MF_FAT) and biological
processes (GOTERM_BP_FAT) categories selected.

Cytokine Antibody Array

Conditioned media were collected from CDCs (7 good and 5 poor
supporters of angiogenesis) after culturing in EGM-2 media for 48
hours. EGM-2 media incubated for 48 hours in fibronectin (0.33
µg/cm^2) coated plates was used as a control. The Proteome Pro-
filer Human XL Cytokine Array Kit (R&D systems) was used accord-
ing to the manufacturer's instructions. Image Studio version 3.1
analysis software was used to determine signal intensity. Signal
intensity for each protein tested was adjusted for the background
intensity of the film and the basal expression level of the condi-
tioned media control.

Migration Assays

Transwells with polycarbonate membranes with 8.0 µm pores
(Appleton Woods) were coated on the top and bottom of the
membrane with fibronectin (0.33 µg/cm^2). 4×10^3 CDCs were
added in 0% fetal bovine serum (FBS, Hyclone) Modified Eagle's
medium (MEM) to the top of the insert and placed into a well
containing 20% FBS MEM. After 24 hours, the transwell insert was
removed and media removed by aspiration. Nonmigratory cells
were removed from the upper surface by wiping with a cotton
bud. The transwell was rinsed in phosphate buffered saline (PBS)
and cells fixed in 4% (wt/vol) Paraformaldehyde and 4% (wt/vol)
Sucrose in PBS. The membrane was rinsed with PBS, cut out from
the transwell and mounted upside down onto a slide using Vecta-
shield mounting media with 4',6-diamino-2-phenylindole (DAPI)
(Vectorlabs, Peterborough, UK, http://www.vectorlabs.com/).
Images were captured at ×100 magnification using an E600
microscope (Nikon), DAPI positive cells were counted using ImageJ
software and the average number of cells per field of view was
calculated for each sample.

Immunocytochemistry

CDCs were fixed with 4% (wt/vol) Paraformaldehyde, 4% (wt/vol)
Sucrose in PBS on culture slides (BD Biosciences). For immunocy-
tochemistry - slides were incubated in target retrieval solution
(Agilent Technologies, Stockport, UK, http://www.agilent.com/) at
95°C for 30 minutes, rinsed in PBS and permeabilized with 0.1%
(vol/vol) Triton X-100, 3% (vol/vol) FBS, before incubation with
Alexa Fluor 647 mouse anti-human Ki-67 (B56) or Alexa Fluor 647
mouse IgG1 κ isotype control (MOPC-21) antibodies (BD Bioscien-
ces) at 4°C, overnight. For proliferation, the Click-iT Alexa Fluor
A488 Imaging kit (Thermofisher, Waltham, MA, USA, http://www.
thermofisher.com/) was used according to the manufacturer's
instructions. Slides were washed in PBS then mounted in Vecta-
shield mounting media with DAPI (Vectorlabs). Images were cap-
tured at ×200 (proliferation) or ×400 (Ki67) magnification using
an E600 microscope (Nikon), stained cells were counted using
ImageJ software.

Western Blotting

Protein lysates were prepared by re-suspending 1×10^7 cell per
milliliter of Radio-Immunoprecipitation Assay (RIPA) buffer;
50 mM Tris-HCl pH 8.0, 150 mM NaCl, 1% (vol/vol) Triton X-100,
0.5% (wt/vol) sodium decoxycholate, 0.1% (wt/vol) sodium
dodecyl sulfate with fresh protease/phosphatase inhibitors (Ther-
mofisher). Samples were incubated on ice for 30 minutes before
clearing the lysate by centrifugation at 12,000 rpm at 4°C for 30
minutes. Protein concentration was determined using the DC Pro-
tein Assay (Bio-Rad). Twenty-five microgram of each protein lysate
was treated with β-mercaptoethanol and separated by electro-
phoresis on 4%–12% NuPAGE Bis-Tris gels (Thermofisher) with
rainbow molecular weight marker (GE Healthcare, Amersham, UK,
http://www.ghealthcare.co.uk/) under reducing conditions. Pro-
teins were transferred to nitrocellulose membranes using an iBlot
(Thermofisher) before blocking with Odyssey Blocking Buffer (LI-
COR, Cambridge, UK, http://www.licor.com/). The membranes
were incubated with rabbit anti-caspase 3 (8G10), rabbit anti-
PARP, rabbit anti-p21 (12D1), rabbit anti-Phospho-RB (D20B12)
mouse anti-RB (4H1) (Cell Signaling Technologies, Leiden, Belgium,
http://www.cellsignal.com/) anti-p53 (FL-393, Insight Biotechnolo-
gies, Wembley, UK, http://www.insightbio.com/) or rabbit anti-
p16-INK4A (Protein tech, Manchester, UK, http://www.protein-
technologies.com/) antibodies. Mouse anti-α-tubulin or mouse
anti-GAPDH antibodies (Sigma, Gillingham, UK, http://www.sig-
maaldrich.com/) were used as loading controls. The appropriate
conjugated secondary antibodies were used for detection before
visualizing using the Odyssey CLx system (LI-COR). Signal intensity
above background was measured using the Odyssey CLx system,
protein levels were standardized to loading controls using Micro-
soft Excel.

Apoptosis

To induce apoptosis CDCs were treated with 400 µg/ml hygromy-
cin (Sigma) for 48 hours, control cells were treated with the same
volume of dimethyl sulfoxide (DMSO). Detached and adherent
cells were lysed in RIPA buffer and prepared for Western blotting
as described previously.

Senescence

CDCs were grown for 72 hours to be approximately 50% conflu-
ent; cells were fixed and stained using the Senescence β-
Galactosidase Staining Kit (Thermofisher) according to the manu-
facturer's instructions. The protocol was amended to reduce the
cell staining time from 12 hours to 8 hours to minimize the num-
ber of false positive cells. Images were captured at ×100 using a
TE2000-U microscope (Nikon) and cells were counted using
ImageJ software.

Animals and Cell Transplantation Procedures

All animal experiments were conducted following ethical approval
by the Centro de Investigación Príncipe Felipe Research Commit-
tee, Valencia, Spain. Care of animals was in accordance with insti-
tutional guidelines. The ischemic disease model was established
as described previously [27–29]. Ligation of the left anterior
descending (LAD) coronary artery was performed on six- to eight-
week-old athymic nude rats (HIH-*Foxn1 rnu,* Charles River Labora-
tories, Inc., Lyon, France, http://www.criver.com/) under appropri-
ate anesthesia and analgesia. Following LAD ligation, animals
were divided into three groups to receive: CDC from good
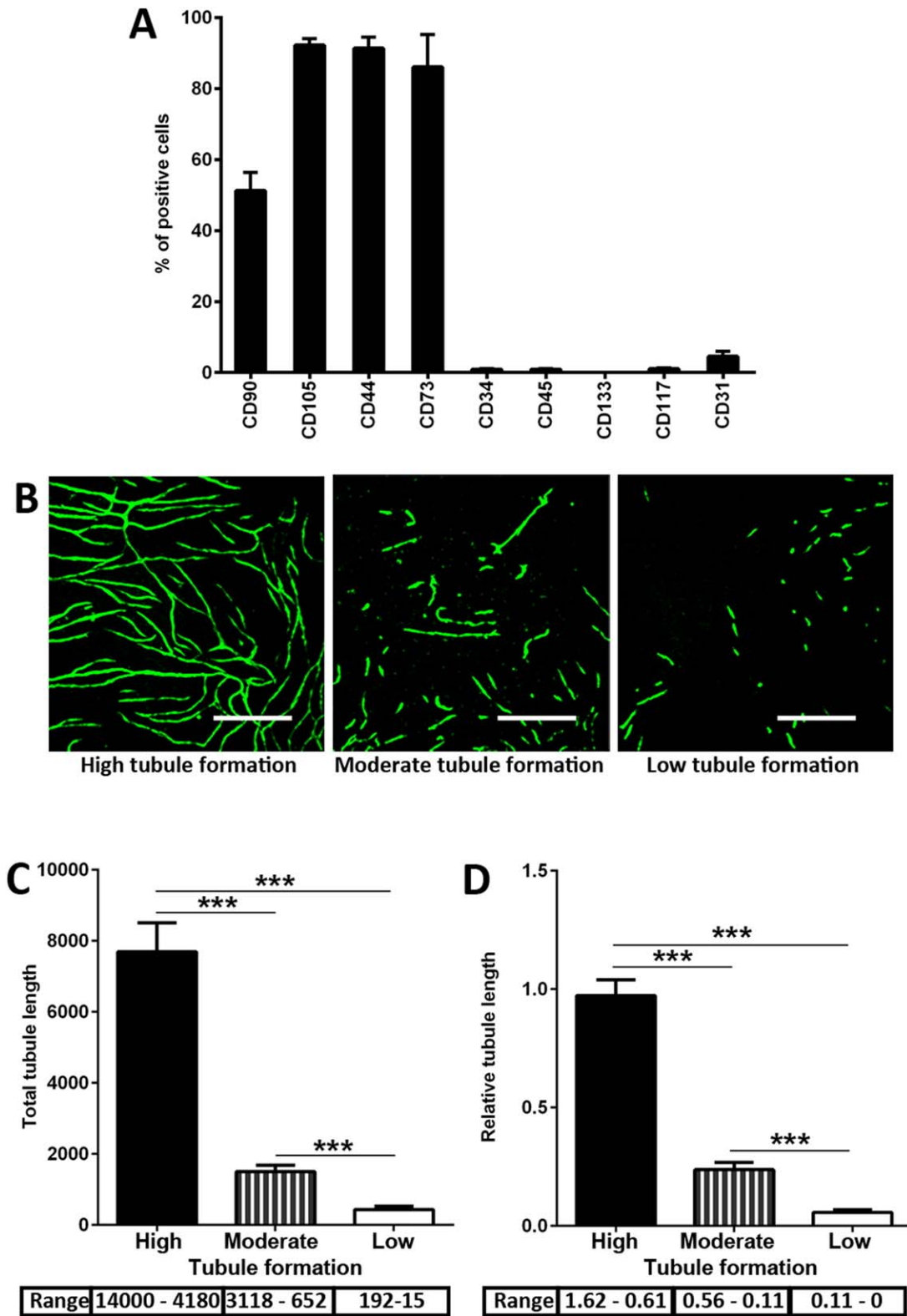
Figure 1. Cardiosphere-derived cells (CDCs) vary in their supportive ability. **(A)**: The immunophenotype of human CDCs extracted from patients with ischemic heart disease (IHD) was analyzed by flow cytometry. The total tubule length (TTL) of GFP-labeled human umbilical vein endothelial cells (HUVECs) was measured after 14 days of coculture with CDCs samples from a total of 43 IHD patients. TTL compared with control supportive cells BMSC was recorded as relative tubule length (RTL). CDC samples patients were subgrouped into three tertiles based on their TTL and RTL, the first tertile was defined as high tubule formation ($n = 14$), the second as moderate tubule formation ($n = 14$), and the third as low tubule formation ($n = 15$) **(B–D)**. (B): Representative images of HUVEC tubule formation after 14 days of coculture with CDCs with high, medium and low tubule formation. Scale bars are equal to 500 μm. Quantification of TTL (C) and RTL (D) for the CDC tertiles with the ranges shown below each graph. Data is presented as mean and standard error of the mean. ***, p value $\leq .001$.

supporters (8 animals), CDC from poor supporters (9 animals), or saline solution (8 animals). Each animal receiving a cell transplant was injected with CDC from one donor; several donors were used for the experiments. The intramyocardial transplantation was performed seven days after the LAD ligation in rats that had sub-acute MI. Animals were infused with 20 μl saline or 1×10^6 cells per animal and fluorescent microspheres (FluorSpheres; 1 μm red fluorescent (580/605) polystyrene microspheres, Thermofisher) diluted 1:40 to visualize the site of injection after tissue processing. For this purpose, three injections were performed at three different points around the infarct zone with a Hamilton syringe (Teknokroma, Barcelona, Spain, http://www.teknokroma.es/en).

Functional assessment was performed at baseline, 15 days and 30 days following cell or saline injections by echocardiography as described elsewhere [27–29]. Briefly, rats were anesthetized and transthoracic echocardiography was performed in a blinded manner using a General Electric system (Vivid 7; GE Healthcare) equipped with a 10-MHz linear-array transducer. Left ventricular (LV) end-systolic and end-diastolic parameters including diameters, areas, anterior wall and septum thickness were measured on two-dimensional and M-Mode echocardiograms at the level of the papillary muscles in the parasternal short axis view, and were used to derive cardiac function values according to the formulas in the Supporting Information methods.

Thirty days post-transplantation the rats were sacrificed, the hearts excised and prepared for immunohistochemistry. Vessel density was determined by immunohistochemistry using a rabbit anti-caveolin-1 antibody (Thermofisher) and an Alexa Fluor 488 conjugated secondary antibody. Masson's trichrome staining was used to assess the remodeling in the left ventricles, as previously described [27].

Statistical Analysis

Differences between three groups (tertiles of TTL and RTL, animal experiments) were estimated using one-way ANOVA test and post hoc two-tailed Student's t test. For experiments comparing CDCs with and without hygromycin treatment, one-tailed Student's t test was used. For all other statistical analyses two-tailed Student's t test was used. p values $\leq .05$ were considered statistically significant.

A multiple regression model was fitted (using R2.15.1 software package) following a Box-Cox transformation to achieve normality of TTL as the λ dependent variable. Age, sex, New York heart association (NYHA) heart function class, type of disease (including exact diseased coronary arteries), comorbidity of hypertension, diabetes, and hypercholesterolemia were used as independent variables. The adjusted coefficient of determination (R-squared) was calculated and the analysis was validated by standard diagnostics of the model's residuals. Clinical data was from 35 patients. Graphs were produced using GraphPad Prism version 6.0 software (GraphPad, La Jolla, Ca, USA, http://www.graphpad.com/).

RESULTS

CDC Vary in Their Ability to Support Endothelial Tubule Formation

CDCs were isolated from patients with IHD undergoing elective CABG (Supporting Information Table S1). CDCs expressed high levels of mesenchymal markers (CD105, CD44, and CD73), were

Table 1. Independent predictors of the pro-angiogenic potential of CDCs

Coefficients		Estimate	SE	t value	p value
(Intercept)		9.218	6.8	1.356	.1874
Age		−0.101	0.083	−1.219	.2344
NYHA class		2.636	1.105	2.385	.0250 *
Type of disease	AS	7.519	3.581	2.099	.0461 *
	CAD	6.703	3.631	1.846	.0768
	Others (VR)	as control			
Diseased RCA		6.558	2.507	2.616	.0149 *
Family history		1.866	1.244	1.5	.1462
Smoking history		5.289	1.974	2.68	.0129 *
Diabetes mellitus		−3.364	2.295	−1.466	.1552
Hypertension		−7.327	2.148	−3.411	.0022 **

		Residuals		
Min	**1Q**	**Median**	**3Q**	**Max**
−8.2	−3.3	0.3	2.7	7.9

Residual standard error: 4.8 on 25 degrees of freedom
Multiple R^2: 0.64, Adjusted R^2: 0.51
F-statistic: 5.0 on 9 and 25 DF, p value: $< .001$

A multiple regression model was used to assess whether there was any independent variable among the correspondent cardiovascular risk factors to predict pro-angiogenic ability of CDCs. The total tubule length was used as the dependent variable in the model, clinical characteristics we used as independent variables. Several clinical characteristics were found to be indicative of CDC supportive ability.
Abbreviations: AS, aortic stenosis; CAD, coronary artery disease; CDC, cardiosphere-derived cell; NYHA, New York heart association; RCA, right coronary artery; SE, standard error; VR, valve replacement.
*, p value $\leq .05$; **, p value $\leq .01$.

positive for CD90 and negative for endothelial (CD31), hematopoietic (CD34, CD45, and CD133) and stem cell (CD117/c-kit) markers in agreement with previous results [6–10, 30] (Fig. 1A, Supporting Information Fig. 1).

Although CDCs can support vessel formation in vivo [7, 17, 18], no previous study has investigated variations in CDCs vascular supportive function among IHD patient samples as a measure of potency. In order to test this in vitro CDCs were cocultured with GFP-labeled HUVECs. The ability of CDCs to support HUVEC tubule formation visibly varied across the patient sample population (Fig. 1B). TTL and RTL were quantified for 43 CDC IHD patient samples, the cohort was then stratified and grouped into tertiles with classifications of high, moderate and low tubule formation (Fig. 1C, 1D). TTL and RTL were significantly different between all three groups of tubule formation ability (Fig. 1C, 1D, all comparisons p value $\leq .001$). Despite their varying vascular supportive ability, no significant difference in key cell surface markers (CD31, CD34, CD45, CD90, CD105, CD117, and CD133) was observed between CDCs with high, moderate or low tubule formation (Supporting Information Table S2).

Cardiovascular Risk Factors Can Partially Predict CDC Vascular Supportive Potential

To determine whether the vascular supportive ability of CDCs could be predicted by disease state or associated risk factors a multiple regression model was established. In this model, TTL was used as a dependent variable and demographic and clinical characteristics were included as independent variables (Table 1). The parameters NYHA class, aortic stenosis, diseased right coronary artery and history of cigarette smoking were found to be significant positive independent predictors of CDCs vascular supportive
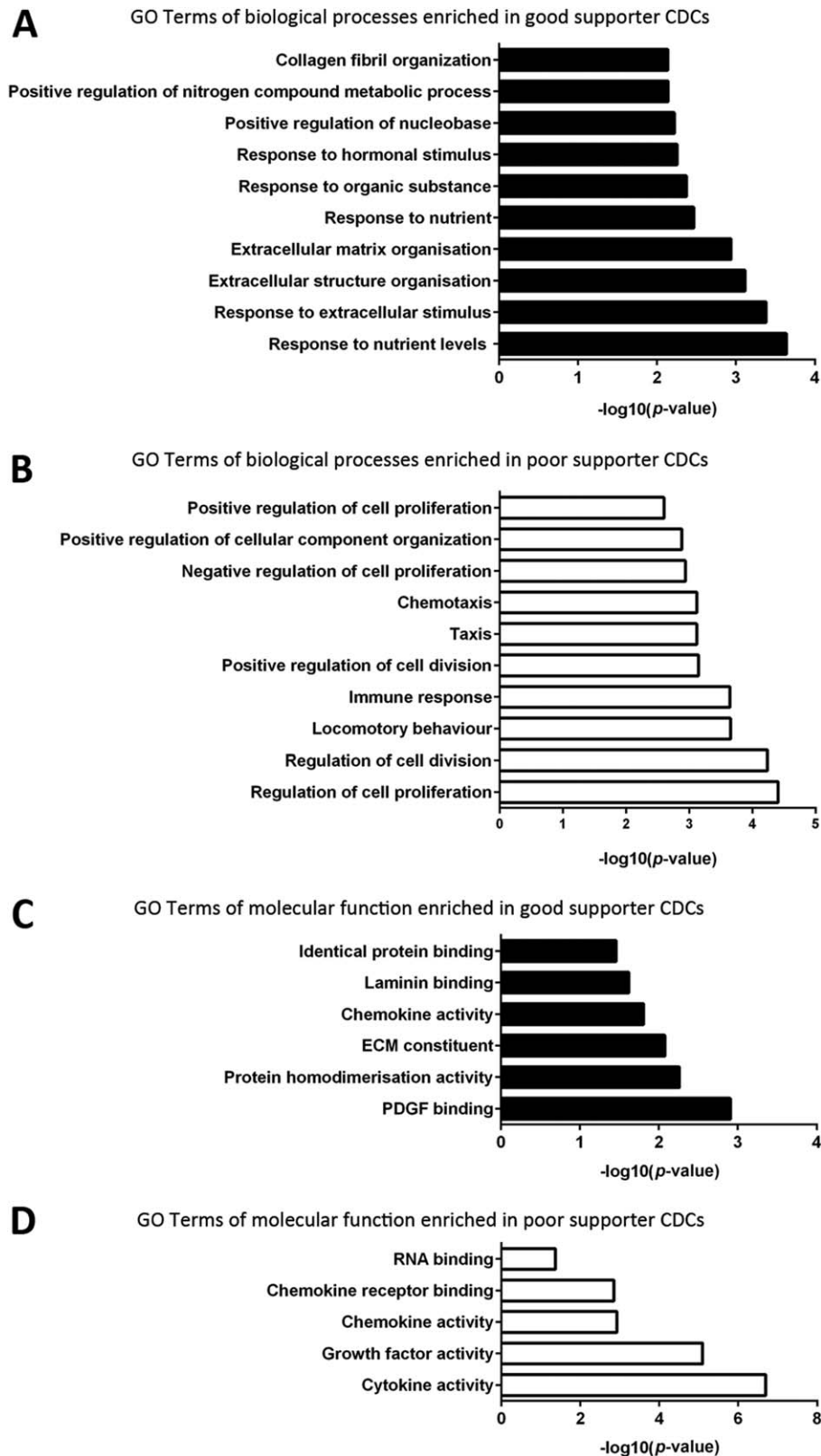
Figure 2. Good and poor supporter CDCs may differ in their structural organization and cytokine release profile. Genes and transcripts highlighted by RNA-sequencing (RNA-seq) as having a differential expression with a posterior probability cut-off of $>.3$ were analyzed by the online tool DAVID. The top 10 significantly upregulated (p value $\leq .05$) biological processes **(A, B)** and molecular functions **(C, D)** categories are shown. Full RNA-seq data can be accessed at gene expression omnibus; accession number GSE81827 (http://www.ncbi.nlm.nih.gov/geo/query/acc.cgi?token=mfupcoyovzyxdub&acc=GSE81827). Abbreviations: CDCs, cardiosphere-derived cells; ECM, extracellular matrix; GO, gene ontology; PDGF, platelet derived growth factor.
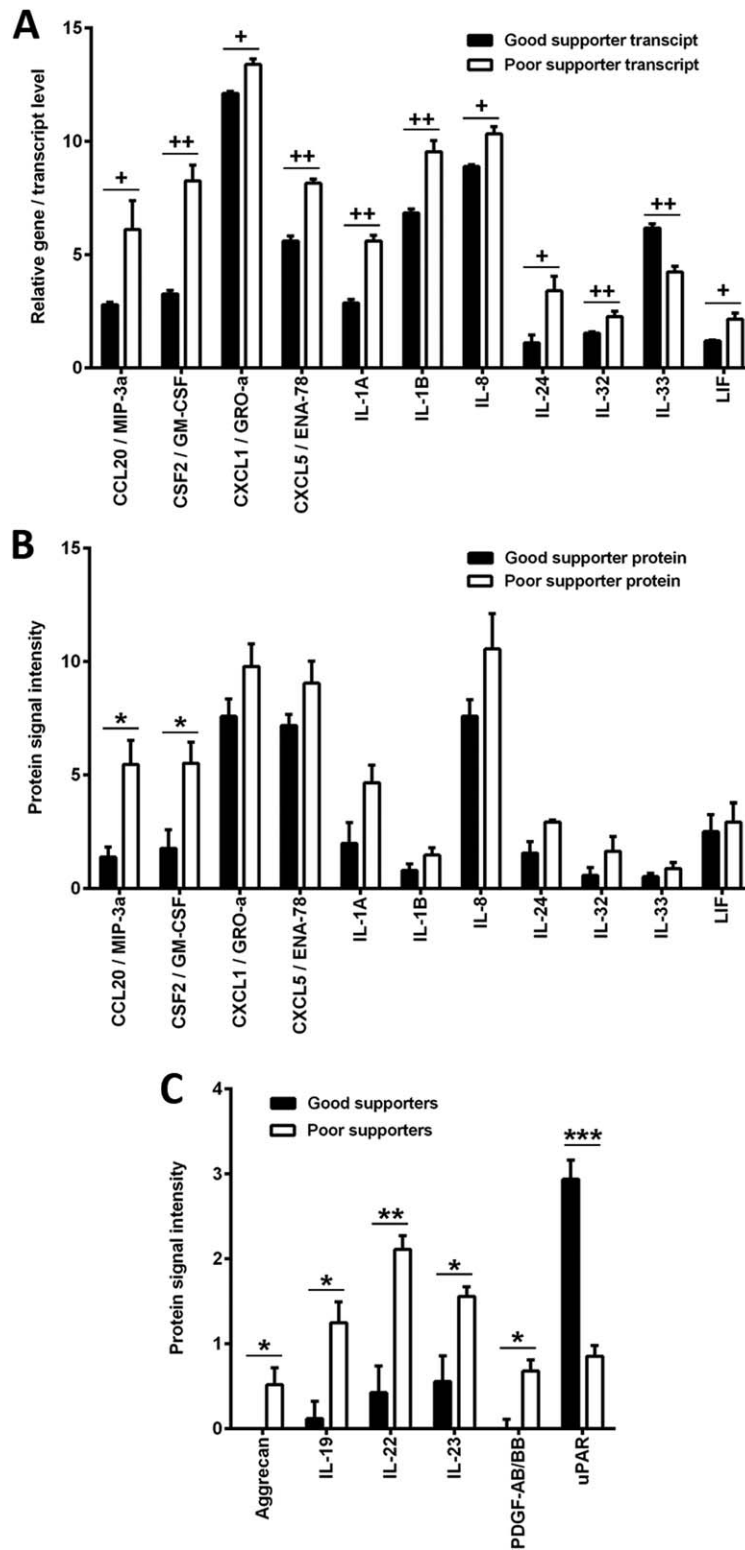
Figure 3. Poor supporter cardiosphere-derived cells (CDCs) have an enhanced inflammatory profile. The expression of 102 cytokines was determined by a human cytokine antibody array, 11 cytokines detected by the array had a differential expression between good and poor supporters in the RNA-sequencing (RNA-seq) array (posterior probability >.3) Gene / transcript levels **(A)** and protein levels **(B)** of the 11 overlapping cytokines are shown for good and poor supporter CDCs. **(C):** Six additional cytokines were significantly different between good and poor supporter CDCs as detected by the cytokine array. For figure A gene levels are shown for all cytokines except IL-32 where transcript data is shown. Data is presented as mean and standard error of the mean. +,posterior probability ≥.3; ++, posterior probability ≥.5; *, p value ≤ .05; **, p value ≤ .01; ***, p value ≤ .001. Full RNA-seq data for (A) can be accessed at gene expression omnibus; accession number GSE81827 (http://www.ncbi.nlm.nih.gov/geo/query/acc.cgi?token=mfupcoyovzyxdub&acc=GSE81827). Abbreviations: PDGF-AB/BB, platelet derived growth factor AB/BB; uPAR, urokinase receptor.

potential. In contrast, hypertension was a significant negative predictor of the ability of CDCs to form tubules (Table 1). The final model accounted for over 51% of the variability in the data ($R^2 = 0.51$).

### Differential Gene and Cytokine Expression in CDCs

To simplify subsequent analysis, CDCs with a TTL above 4,000 were referred to as good supporters of angiogenesis (good supporters) and CDCs with a TTL below 4,000 were referred to as poor supporters of angiogenesis (poor supporters).

Differential gene expression between good and poor supporter CDCs was assessed by RNA-seq. Using a posterior probability of >.3, we identified 54 genes and 88 transcripts upregulated in good supporters compared to 58 genes and 76 transcripts upregulated in poor supporter CDCs. Biological processes enriched in good supporters related to nutrient response and extracellular components (Fig. 2A, Supporting Information Table S3), while in poor supporters, they related to the immune response, cell proliferation, cell division and migration (Fig. 2B, Supporting Information Table S3). Enriched molecular functions in good supporters related to extracellular signaling (Fig. 2C, Supporting Information Table S4), while in poor supporters they related to inflammatory signaling (Fig. 2D, Supporting Information Table S4). The categories highlighted by the gene ontology (GO) analysis suggested that good and poor supporter CDCs will differ in their structural organization of the extracellular matrix (ECM) and cytokine release profile.

To validate the latter, cytokine secretion by good and poor supporter CDCs was assessed using an antibody array platform (Supporting Information Fig. S2). Differences between good and poor supporters were observed for 11 cytokines that had shown differential gene expression by RNA-seq (Fig. 3A, 3B). The gene and protein data from the RNA-seq and cytokine arrays for the 11 cytokines were compared (Fig. 3A, 3B), the majority of the targets had the same trend and two were significantly higher in poor supporters at the gene and protein level (CCL20/Mip-3a and CSF2/GM-CSF). The cytokine arrays highlighted six additional cytokines which were significantly different between good and poor supporter CDCs (Fig. 3B, 3C). Mip-3a, GM-CSF, Aggrecan, Interleukin (IL)-19, IL-22, IL-23, and platelet derived growth factor AB/BB were significantly upregulated in poor supporters, while urokinase receptor was significantly upregulated in good supporters (Fig. 3C). Overall, these data suggest that the poor supporters secrete an increased amount of inflammatory cytokines.

Good and Poor Supporter CDCs Differ in Their Proliferation and Cell Cycle Progression but not in Migratory Ability

"Locomotory behavior," "Taxis," "Chemotaxis," "Cell division," and "Cell proliferation" were enriched biological process in poor supporters (Fig. 2B). However, there was no difference in migratory ability of the CDCs tested by a Boyden chamber migration assay (Fig. 4A). Three different assays were used to assess cell proliferation and cell cycle progression; 5-ethynyl-2′-deoxyuridine (EdU) incorporation, Ki67 expression and phosphorylation state of the retinoblastoma (Rb) protein, a crucial regulator of the cell cycle. EdU staining determined that good supporter CDCs had approximately three times more cells actively proliferating compared to poor supporter CDCs (Fig. 4B, p value = .014). This was confirmed by expression of Ki-67 being detected in 50.61% of good supporter CDCs and 16% of poor supporter CDCs, indicating that cell cycle
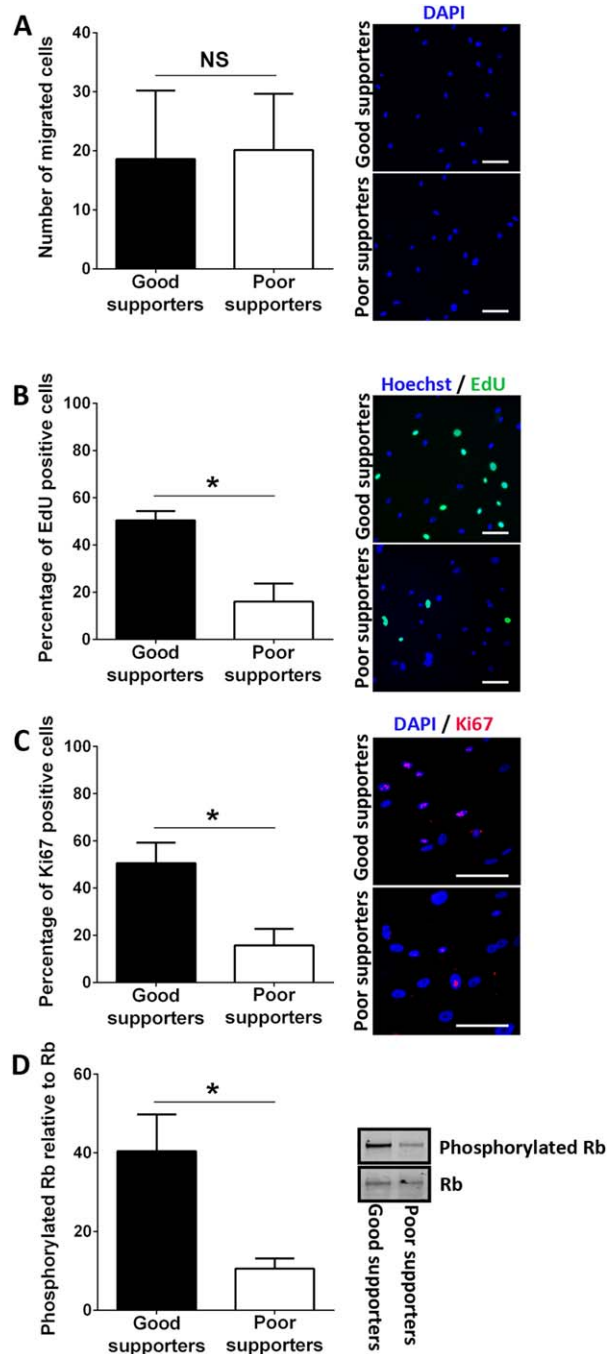
Figure 4. Poor supporter cardiosphere-derived cells (CDCs) have reduced proliferation and cell cycle progression but do not differ in migratory ability compared to good supporter CDCs. **(A)**: Migratory ability of CDCs as shown by the mean number of CDCs which had migrated through a transwell with 8 μm pores toward a serum gradient after 24 hours of culture, with representative images (×100). **(B)**: Quantification of the percentage of EdU positive CDCs with representative images (×200) as measured by a Click-iT proliferation assay. **(C)**: Quantification of Ki67 positive CDCs with representative images (×400). **(D)**: Quantification of the phosphorylated and non-phosphorylated form of Rb in CDCs with good and poor supportive potential, with representative images. Scale bars are equal to 100 μm. Data is presented as mean and standard error of the mean. *, p value ≤ .05. Abbreviations: DAPI, 4′,6-diamino-2-phenylindole; NS, non-significant; EdU, 5-ethynyl-2′-deoxyuridine; Rb, retinoblastoma.

progression was significantly lower in poor supporter CDCs (Fig. 4C, *p* value = .018). Finally, in agreement good supporter CDCs had a significantly higher level of phosphorylated Rb compared to poor supporters (Fig. 4D, *p* value = .031), indicating that cell cycle progression is reduced in poor supporter CDCs. Together, these findings show that the ability for CDCs to progress through the

cell cycle and proliferate is significantly diminished in poor supporter CDCs.

Poor Vascular Supportive Function Is Associated with Resistance to Apoptosis and Senescence

Due to the reduced proliferative capacity of poor supporter CDCs, we hypothesized that these cells may be undergoing apoptosis. Cleaved caspase 3 and cleaved poly(ADP-ribose) polymerase (PARP) are well established markers of early and late apoptosis, respectively [31, 32]. There were no significant differences between good and poor supporter CDCs in the expression levels of caspase 3 (full length or cleaved) or full length PARP at basal levels (DMSO treated, Fig. 5A–5F). However, at basal levels cleaved PARP was five times higher in poor supporter CDCs than in good supporter CDCs (Fig. 5F), this was found to be due to 2 of the 4 poor supporters having relatively high levels of cleaved PARP (Fig. 5A, lane 5). This finding indicated that there may be a higher level of late apoptosis in some poor supporter CDCs.

Hygromycin treatment induces both early and late apoptosis in mammalian cells by blocking the elongation step of translation [33]. Hygromycin stimulates the cleavage of both caspase 3 and PARP, this process was seen in the CDCs tested but the strength of the response varied between good and poor supporters. The expression levels of caspase 3 and PARP were compared in DMSO and hygromycin treated CDCs. Despite a general trend of decreased full length and increased cleaved fragments of Caspase 3 and PARP, the only significant change was in the downregulation of full length caspase 3 in good supporter CDCs (Fig. 5B, *p* value = .045). In contrast, the levels of full length caspase 3 in poor supporters were unchanged after hygromycin treatment (Fig. 5B). Good supporters produced a large increase of the cleaved caspase 3 fragments in response to hygromycin (Fig. 5C, 5D), poor supporters also responded to hygromycin but the effect was approximately four times lower than in good supporter CDCs (Fig. 5C, 5D). Similarly, good supporters induced a large increase in the cleaved fragment of PARP in response to hygromycin (~15-fold increase), whereas poor supporters were less efficient and only increase the expression of cleaved PARP by approximately two-fold after hygromycin treatment (Fig. 5F). Therefore, poor supporter CDCs had a reduced response to pro-apoptotic stimuli compared to good supporter CDCs, suggesting a resistance to apoptosis.

Taken together, the enhanced inflammatory cytokine profile, reduced proliferative rates and resistance to apoptotic insult are hallmarks of cellular senescence [34, 35]. When CDCs were stained
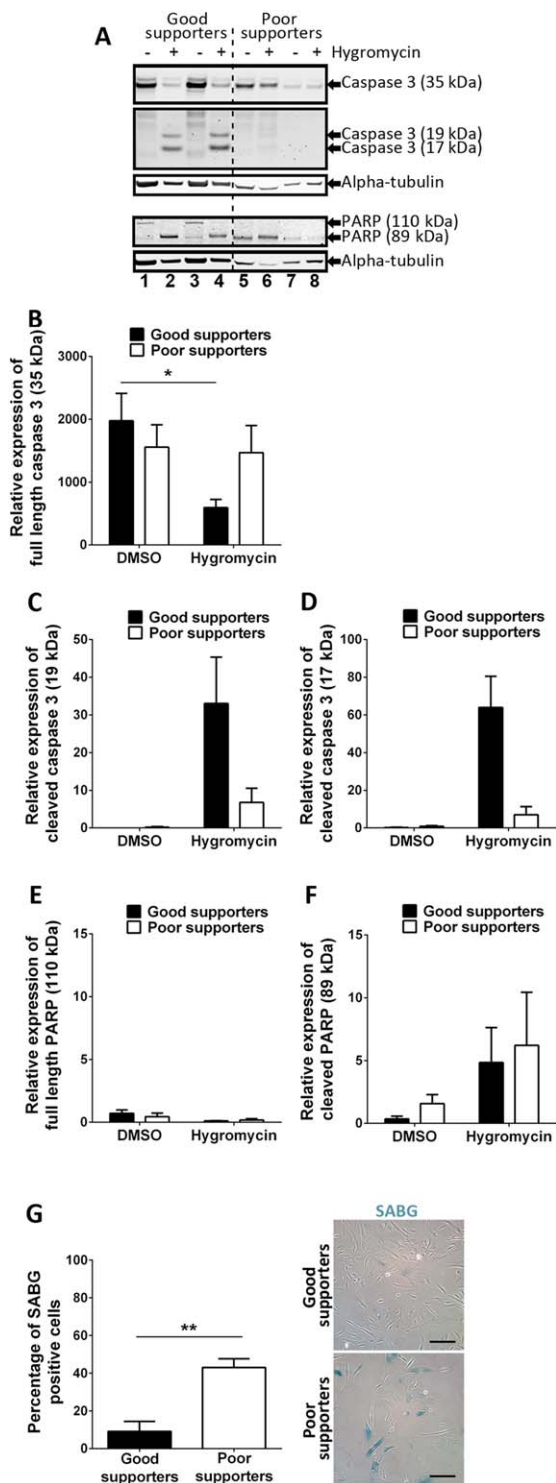

Figure 5.

Figure 5. Poor supporters are resistant to apoptosis and have increased levels of senescence. Early and late apoptosis were measured in good and poor supporter cardiosphere-derived cells (CDCs) by analysis of total and cleaved caspase 3 and PARP protein levels. Apoptosis was induced by hygromycin treatment and compared to control DMSO treated CDCs. **(A)**: Representative images of caspase 3 and PARP Western blots. Quantification of full length [35 kDa, **(B)**] and cleaved [19 kDa **(C)**, 17 kDa **(D)**] caspase 3. Quantification of full length [110 kDa, **(E)**] and cleaved [89 kDa, **(F)**] PARP. **(G)**: Quantification of senescence associated β-galactosidase (SABG) positive CDCs with representative images (×100). Scale bars are equal to 200 μm. Data is presented as mean and standard error of the mean. *, *p* value ≤ .05; **, *p* value ≤ .01. Abbreviations: DMSO, dimethyl sulfoxide; PARP, poly(ADP-ribose) polymerase; SABG, senescence associated β-galactosidase.

for senescence associated β-galactosidase (SABG), poor supporter CDCs were found to have a significantly higher number of positive cells, suggesting these cells are senescent (Fig. 5G, p value = .0086). To determine which senescent pathways were differentially regulated in poor supporters, levels of three classical senescence markers; p16, p21, and p53 were investigated. Surprisingly, there were no differences in the three senescence markers between good and poor supporter CDCs (Supporting Information Fig. S3). p16, p21, and p53 were expressed ubiquitously in the CDCs tested, irrespectively of their vascular supportive ability. These data suggest that CDCs with poor supportive function are senescent but classical senescence markers are not suitable for detecting senescence in this cell type.
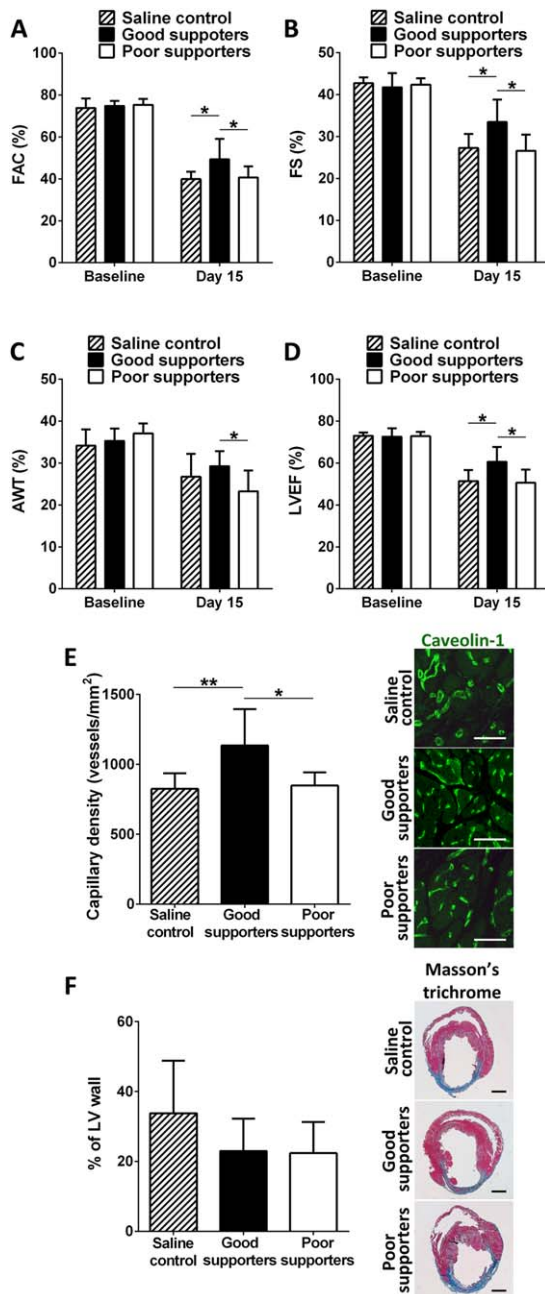
Vascular Supportive Function In Vitro Correlates with Therapeutic Potential In Vivo

To test the hypothesis that the differences in supportive CDC function observed in vitro can represent their therapeutic potential, a preliminary in vivo study was conducted. MI was induced by LAD ligation in athymic nude rats (HIH-*Foxn1 rnu*) and good supporter CDCs, poor supporter CDCs or a saline control were injected into the rat myocardium. Cardiac functional parameters were assessed at baseline, day 15 and day 30 to evaluate the functional recovery (Fig. 6, Supporting Information Fig. S4). Systolic function estimated by percentage of fractional area change (FAC) was significantly improved by infusion of good supporter CDCs compared to control at day 15 (Fig. 6A, p value = .031). Fractional shortening (FS) improved following injection of good supporter CDC at day 15 when compared to control (Fig. 6B, p value = .017). Infusion of good supporter CDCs improved systolic function measured by FAC or FS when compared to poor supporters (Fig. 6A, 6B, FAC p value = .48, FS p value = .012). Poor supporter CDCs had no significant effect on FAC or FS compared to saline control (Fig. 6A, 6B, FAC p value = .745, FS p value = .728). Changes in the anterior wall of the left ventricle (LV) were measured as a percentage of aortic wall thickness (AWT), at day 15 animals injected with good supporter CDCs had a significantly higher AWT than animals injected with poor supporter CDCs (Fig. 6C, p value = .017). However, the difference between the good supporters and saline treatment groups was not significant (Fig. 6C, p value = .295). Surprisingly, the AWT percentage in rats treated with CDCs from the poor supporters seemed to be worse than in the saline treated groups (Fig. 6C, p value = .208). Finally, infusion of good supporter CDCs significantly improved EF at day 15 when compared to the saline group or poor supporter CDC infusion (Fig. 6D, vs. saline p value = .012 vs. poor p value = .011). No changes in EF were detected after infusion with poor supporter CDCs when compared to the saline control (Fig. 6D, day 15 p value = .793).

Angiogenesis, measured by capillary vessel density in the LV was significantly improved by good supporter CDC infusion compared to the saline control (Fig. 6E, p value = .005). In contrast, animals injected with poor supporter CDCs did not show a

Figure 6.

Figure 6. Effect of cardiosphere-derived cell (CDC) transplantation on LV function, capillary density and infarct size. Adult athymic (HIH-*Foxn1rnu*) rats had the left anterior descending LAD artery ligated. Animals were split into three groups which received either CDCs from good supporters, CDC from poor supporters or saline as a control. Echocardiography was used to measure heart function at baseline and 15 days. **(A)**: Percentage of fractional area change (FAC %). **(B)**: Percentage of fractional shortening (FS %) change. **(C)**: Percentage of anterior wall thickening (AWT %). **(D)**: Percentage change in left ventricular ejection fraction (LVEF %). 30 days following transplantation of CDCs or saline the hearts were excised, sectioned and stained with anti-caveolin antibody or with Masson's trichrome stain. **(E)**: Quantification of capillary density (vessels/mm^2) in the hearts of animals infused with good supporters, poor supporters or saline control as measured by caveolin immunostaining, with representative images (×200, scale bars are equal to 50 μm). **(F)**: Quantification of infarct size (% of LV wall) in the hearts of animals infused with good supporters, poor supporters or saline control as measured by Masson's trichrome stain, with representative images (scale bars are equal to 2 mm). In (F), the fibrotic tissue around the infarct stains blue against the healthy myocardium in red. Data is presented as mean and standard error of the mean. *, p value ≤ .05; **, p value ≤ .01. Abbreviations: AWT, aortic wall thickness; FAC %, percentage of fractional area change; FS %, percentage of fractional shortening; LVEF, left ventricular ejection fraction.

significant change in vessel density compared to animals injected with saline (Fig. 6E, *p* value = .817). Animals treated with good or poor supportive CDCs showed a reduction of the fibrotic scar size compared to control animals, but this trend was not significant (Fig. 6F, good *p* value = .92, poor *p* value = .064). These results suggest that CDCs from both groups can partially reduce the fibrotic scar to the same extent, but only those with a robust angiogenic potential increase vessel density and improve systolic function in the ischemic heart.

DISCUSSION

The variable results obtained in cardiac regenerative cell therapy trials call for a personalized approached to cell therapy and the need to develop better potency assays. Therefore, it is crucial to select the optimal cell type and the best responder patient population who would benefit most from such therapies. In this study, CDCs were isolated and expanded from a cohort of patients undergoing elective cardiac surgery reflective of the epidemiology of cardiovascular disease [36]. To our knowledge, this is the first time that therapeutic potential due to differences in the CDC's vascular supportive ability have been reported in this patient cohort. CDCs were grouped according to their ability to support vascular tubule formation in vitro. Traditionally, the expression of single cell surface markers that could define a therapeutic cell population has been sought. Recently, the expression of CD90 has been associated with the therapeutic potential of CDCs in humans [37]. However, in the current study the supportive ability of CDCs did not correlate with CD90 expression or indeed any other cell surface marker tested. A multiple regression model used to link CDCs' vascular supportive ability with donor characteristics indicated patients with advanced disease state (higher NYHA class, aortic stenosis and diseased right coronary artery) and/or were previous smokers were more likely to produce good supporter CDCs, while hypertension appeared to be a significant negative predictor of CDCs vascular supportive function. This is in agreement with recent studies suggesting that CDCs from adult and pediatric patients with advanced heart failure outperformed CDCs from healthy donor hearts or control heart disease when tested in a rodent model of MI [7, 38]. In our study, hypertension is a significant negative independent predictor of CDCs' vascular supportive ability. A new report has suggested that offspring born to hypertensive mothers have reduced vasculogenic potential at birth and this correlates with loss of microvessel density over the first three months of life [39], which suggest a correlation between in vitro and in vivo vascular development. Patients included in our study were neither treated with the isolated CDCs nor were they followed-up to monitor collateral vessel development. However, it is plausible that patients who yield poor supporters CDCs may have impaired collateral growth development.

Molecular analysis carried out in our study revealed only a small number of differentially expressed genes and transcripts between good and poor supporter CDCs. This was not surprising as IHD is a common complex polygenic disease involving a combination of multiple genes, each contributing with small effects on the phenotype, therefore it is important to identify functional biomarkers that correlate with cell potency. In our study, poor supporter CDCs were found to have reduced proliferative potential, variability in CDCs growth patterns has previously been observed but not necessarily associated to their therapeutic potential [8,

40]. In addition to reduced proliferative potential, poor supporter CDCs were resistant to apoptotic stimuli and secreted higher amounts of inflammatory cytokines, all of which are hallmarks of cell senescence [34, 35]. The cell senescence associated secreted profile (SASP) is thought to be a stress response to signal for repair and has been well characterized [34, 35, 41]. Interestingly, several of these factors (inflammatory cytokines) were significantly higher in poor supporter CDCs at the mRNA (RNA-seq; CXCL1/GRO-a, IL-1A, IL-1B, IL-8) and protein (cytokine array; GM-CSF, CCL20/MIP-3a) level. Cell stress induces a complex response and it is unknown why some cells undergo apoptosis and others induce or undergo senescence. The outcome will most likely depend on the cell type, DNA damage, genetic differences between donors and previous environmental stresses and insults to which the cell has been exposed [35, 42]. In addition to the increased SASP in poor supporters, these cells expressed high levels of SABG. However, the expression of classic senescent markers p16, p21, and p53 were similar in good and poor supporter CDCs. This may be due to the cell samples originating from patients of advanced age with IHD, as both states can increase senescent markers [42, 43]. Recently, a slight increase in SABG in CDCs from older patients has been observed [30]. However, as in our study, the senescence markers p16, p21, and p53 were expressed in the majority of CDCs tested and did not correlate with SABG levels [30]. The presence of senescence in CDCs may be a positive, as loss of these markers can indicate immortalization and oncogenesis [35, 44]. Collectively, these findings are particularly important for cell therapy as previous studies in the field have established negative p16 expression as a measure of cell fitness [45]. Our study shows that these markers are not sufficient for detecting senescent CDCs and that the ability to support tubule formation provides a better insight into functional and therapeutic ability.

Results obtained in vitro using such functional assays have been confirmed in vivo in a preclinical model of MI. We have demonstrated that transplantation of good supporter CDCs diminishes ventricular remodeling compared to poor supporters or saline, they significantly improved systolic function in the rat model of MI. Vascular supportive ability of CDCs tested in vitro was a predictive measure of improved capillary density in vivo. Animals transplanted with CDCs showed a reduction of infarct size irrespective of supportive potential, although this was not significant. Taken together these results suggest that only CDCs with robust pro-angiogenic ability improved LV remodeling, systolic function and capillary density. Cell senescence has previously been shown to prevent MSC cell therapy rescue in an LPS-induced lethal endotoxemia study [41] and reduced the therapeutic effect of CPC when infused into a mouse model of MI [46].

CONCLUSION

In this study, CDCs classed as poor supporters had a reduced capability to support HUVEC tubule formation, an increased inflammatory profile, decreased proliferation, were resistant to apoptotic insult and had a higher proportion of senescent cells. By contrast, good supporter CDCs had a robust vascular supportive ability and high proliferative potential. The tubule assay highlighted the difference between good and poor supporter CDCs from patients with IHD and was predictive of in vivo outcomes; it could therefore be used as a potency assay for cell therapy. Assessing cell potency is crucial to the success of cell therapies and while

patients who could provide potent therapeutic cells could be amenable to autologous transplantation, those providing cells with impaired therapeutic potential could benefit from rejuvenation treatments [38, 46–48] or allogeneic cell transplantation [12, 14, 17, 18, 49, 50], enabling a personalized approach to cell therapy and improving outcomes in clinical trials.

AUTHOR CONTRIBUTIONS

E.H.: conception and design, collection and/or assembly of data, data analysis and interpretation, manuscript writing; H.Z. and P.S.: conception and design, collection and/or assembly of data, data analysis and interpretation; S.P.G., D.S., D.C., and G.N.T.: collection and/or assembly of data, data analysis and interpretation; F.A.C., R.P., and D.J.B.: data analysis and interpretation; H.K.: provision of study materials or patients; D.P.T.: financial support, provision of study materials or patients; M.F.: collection and/or assembly of data, data analysis and interpretation; S.M.W.: financial support, data analysis and interpretation, final approval of manuscript; E.M.-R.: conception and design, financial support, data analysis and interpretation, manuscript writing, final approval of manuscript.

DISCLOSURE OF POTENTIAL CONFLICTS OF INTEREST

The authors indicated no potential conflicts of interest.

REFERENCES

1 Velagaleti RS, Pencina MJ, Murabito JM et al. Long-term trends in the incidence of heart failure after myocardial infarction. Circulation 2008;118:2057–2062.

2 World Health Organisation. The top 10 causes of death. Available at http://www.who.int/media centre/factsheets/fs310/en. Accessed April 5, 2016.

3 Yoon CH, Koyanagi M, Iekushi K et al. Mechanism of improved cardiac function after bone marrow mononuclear cell therapy: Role of cardiovascular lineage commitment. Circulation 2010;121:2001–2011.

4 Dimmeler S, Leri A. Aging and disease as modifiers of efficacy of cell therapy. Circ Res 2008;102:1319–1330.

5 Kissel CK, Lehmann R, Assmus B et al. Selective functional exhaustion of hematopoietic progenitor cells in the bone marrow of patients with postinfarction heart failure. J Am Coll Cardiol 2007;49:2341–2349.

6 Chan HH, Meher Homji Z, Gomes RS et al. Human cardiosphere-derived cells from patients with chronic ischaemic heart disease can be routinely expanded from atrial but not epicardial ventricular biopsies. J Cardiovasc Transl Res 2012;5:678–687.

7 Cheng K, Malliaras K, Smith RR et al. Human cardiosphere-derived cells from advanced heart failure patients exhibit augmented functional potency in myocardial repair. JACC Heart Fail 2014;2:49–61.

8 Koninckx R, Daniëls A, Windmolders S et al. Mesenchymal stem cells or cardiac progenitors for cardiac repair? A comparative study. Cell Mol Life Sci 2011;68:2141–2156.

9 Smith RR, Barile L, Cho HC et al. Regenerative potential of cardiosphere-derived cells expanded from percutaneous endomyocardial biopsy specimens. Circulation 2007;115:896–908.

10 Vahdat S, Mousavi SA, Omrani G et al. Cellular and molecular characterization of human cardiac stem cells reveals key features essential for their function and safety. Stem Cells Dev 2015;24:1390–1404.

11 Li TS, Cheng K, Malliaras K et al. Direct comparison of different stem cell types and subpopulations reveals superior paracrine potency and myocardial repair efficacy with cardiosphere-derived cells. J Am Coll Cardiol 2012;59:942–953.

12 Zwetsloot PP, Vegh AM, Jansen Of Lorkeers SJ et al. Cardiac stem cell treatment in myocardial infarction: A systematic review and meta-analysis of preclinical studies. Circ Res 2016;118:1223–1232.

13 Ishigami S, Ohtsuki S, Tarui S et al. Intracoronary autologous cardiac progenitor cell transfer in patients with hypoplastic left heart syndrome: The TICAP prospective phase 1 controlled trial. Circ Res 2015;116:653–664.

14 Malliaras K, Makkar RR, Smith RR et al. Intracoronary cardiosphere-derived cells after myocardial infarction: Evidence of therapeutic regeneration in the final 1-year results of the CADUCEUS trial (CArdiosphere-derived aUtologous stem CElls to reverse ventricular dysfunction). J Am Coll Cardiol 2014;63:110–122.

15 Makkar RR, Smith RR, Cheng K et al. Intracoronary cardiosphere-derived cells for heart regeneration after myocardial infarction (CADUCEUS): A prospective, randomised phase 1 trial. Lancet 2012;379:895–904.

16 Watt SM, Gullo F, van der Garde M et al. The angiogenic properties of mesenchymal stem/stromal cells and their therapeutic potential. Br Med Bull 2013;108:25–53.

17 Chimenti I, Smith RR, Li T et al. Relative roles of direct regeneration versus paracrine effects of human cardiosphere-derived cells transplanted into infarcted mice. Circ Res 2010;106:971–980.

18 Kanazawa H, Tseliou E, Dawkins JF et al. Durable benefits of cellular postconditioning: Long-term effects of allogeneic cardiosphere-derived cells infused after reperfusion in pigs with acute myocardial infarction. J Am Heart Assoc 2016;5. pii: e002796. doi: 10.1161/JAHA.115.002796.

19 Stuckey DJ, Carr CA, Martin-Rendon E et al. Iron particles for noninvasive monitoring of bone marrow stromal cell engraftment into, and isolation of viable engrafted donor cells from, the heart. STEM CELLS 2006;24:1968–1975.

20 Zhang YY, Fisher N, Newey SE et al. The impact of proliferative potential of umbilical cord-derived endothelial progenitor cells and hypoxia on vascular tubule formation in vitro. Stem Cells Dev 2009;18:359–375.

21 Chen L, Kostadima M, Martens JHA et al. Transcriptional diversity during lineage commitment of human blood progenitors. Science 2014;345:1251033–1251031–1251010.

22 Turro E, Astle WJ, Tavare S. Flexible analysis of RNA-seq data using mixed effects models. Bioinformatics 2014;30:180–188.

23 Langmead B, Trapnell C, Pop M et al. Ultrafast and memory-efficient alignment of short DNA sequences to the human genome. Genome Biol 2009;10:R25.

24 Turro E, Su SY, Goncalves A et al. Haplotype and isoform specific expression estimation using multi-mapping RNA-seq reads. Genome Biol 2011;12:R13.

25 Huang DW, Sherman BT, Lempicki RA. Systematic and integrative analysis of large gene lists using DAVID bioinformatics resources. Nat Protoc 2009;4:44–57.

26 Huang DW, Sherman BT, Lempicki RA. Bioinformatics enrichment tools: Paths toward the comprehensive functional analysis of large gene lists. Nucleic Acids Res 2009;37:1–13.

27 Armiñan A, Gandia C, Garcia-Verdugo JM et al. Mesenchymal stem cells provide

better results than hematopoietic precursors for the treatment of myocardial infarction. J Am Coll Cardiol 2010;55:2244–2253.

28 Cerrada I, Ruiz-Sauri A, Carrero R et al. Hypoxia-inducible factor 1 alpha contributes to cardiac healing in mesenchymal stem cells-mediated cardiac repair. Stem Cells Dev 2013;22:501–511.

29 Gandia C, Arminan A, Garcia-Verdugo JM et al. Human dental pulp stem cells improve left ventricular function, induce angiogenesis, and reduce infarct size in rats with acute myocardial infarction. Stem Cells 2008;26:638–645.

30 Nakamura T, Hosoyama T, Kawamura D et al. Influence of aging on the quantity and quality of human cardiac stem cells. Sci Rep 2016;6:1–11.

31 Fernandes-Alnemri T, Litwack G, Alnemri ES. CPP32, a novel human apoptotic protein with homology to Caenorhabditis elegans cell death protein Ced-3 and mammalian interleukin-1 beta-converting enzyme. J Biol Chem 1994;269:30761–30764.

32 Oliver FJ, de la Rubia G, Rolli V et al. Importance of poly(ADP-ribose) polymerase and its cleavage in apoptosis. Lesson from an uncleavable mutant. J Biol Chem 1998;273:33533–33539.

33 Cabaňas MJ, Vazquez D, Modolell J. Dual interference of hygromycin B with ribosomal translocation and with aminoacyl-tRNA recognition. Eur J Biochem 1978;87:21–27.

34 Herranz N, Gallage S, Mellone M et al. mTOR regulates MAPKAPK2 translation to control the senescence-associated secretory phenotype. Nat Cell Biol 2015;17:1205–1217.

35 Childs BG, Baker DJ, Kirkland JL et al. Senescence and apoptosis: Dueling or complementary cell fates? EMBO Rep 2014;15:1139–1153.

36 Ho KK, Pinsky JL, Kannel WB et al. The epidemiology of heart failure: The Framingham Study. J Am Coll Cardiol 1993;22(suppl A):6A–13A.

37 Cheng K, Ibrahim A, Hensley MT et al. Relative roles of CD90 and c-Kit to the regenerative efficacy of cardiosphere-derived cells in humans and in a mouse model of myocardial infarction. J Am Heart Assoc 2014;3:1–10.

38 Sharma S, Mishra R, Simpson D et al. Cardiosphere-derived cells from pediatric end-stage heart failure patients have enhanced functional activity due to the heat shock response regulating the secretome. Stem Cells 2015;33:1213–1229.

39 Yu GZ, Aye CYL, Lewandowski AJ et al. Association of maternal antiangiogenic profile at birth with early postnatal loss of microvascular density in offspring of hypertensive pregnancies. Hypertension 2016;68:749–759.

40 Gago-Lopez N, Awaji O, Zhang Y et al. THY-1 receptor expression differentiates cardiosphere-derived cells with divergent cardiogenic differentiation potential. Stem Cell Reports 2014;2:576–591.

41 Sepúlveda J, Tomé M, Fernández M et al. Cell senescence abrogates the therapeutic potential of human mesenchymal stem cells in the lethal endotoxemia model. Stem Cells 2014;32:1865–1877.

42 Rota M, Goichberg P, Anversa P et al. Aging effects on cardiac progenitor cell physiology. Compr Physiol 2015;5:1775–1814.

43 Cesselli D, Beltrami AP, D'Aurizio F et al. Effects of age and heart failure on human cardiac stem cell function. Am J Pathol 2011;179:349–366.

44 Rubio D, Garcia S, Paz MF et al. Molecular characterization of spontaneous mesenchymal stem cell transformation. PLoS One 2008;3:e1398.

45 Bolli R, Chugh AR, D'Amario D et al. Cardiac stem cells in patients with ischaemic cardiomyopathy (SCIPIO): Initial results of a randomised phase 1 trial. Lancet 2011;378:1847–1857.

46 Avolio E, Gianfranceschi G, Cesselli D et al. Ex vivo molecular rejuvenation improves the therapeutic activity of senescent human cardiac stem cells in a mouse model of myocardial infarction. Stem Cells 2014;32:2373–2385.

47 Hariharan N, Quijada P, Mohsin S et al. Nucleostemin rejuvenates cardiac progenitor cells and antagonizes myocardial aging. J Am Coll Cardiol 2015;65:133–147.

48 Mohsin S, Khan M, Nguyen J et al. Rejuvenation of human cardiac progenitor cells with Pim-1 kinase. Circ Res 2013;113:1169–1179.

49 Makkar R, Schatz R, Traverse JH et al. ALLogeneic heart STem cells to Achieve myocardial Regeneration (ALLSTAR): The six month phase I safety results. J Am Coll Cardiol 2014;64(suppl B):Abstract TCT-152.

50 Makkar R, Schatz R, Traverse J et al. ALLogeneic heart STem cells to Achieve myocardial Regeneration (ALLSTAR): the one year phase I results. Circulation 2014;130(suppl 2):Abstract 20536.

🖥 See www.StemCellsTM.com for supporting information available online.